

Evolution of π^0 suppression in Au+Au collisions from $\sqrt{s_{NN}} = 39$ to 200 GeV

A. Adare,¹¹ S. Afanasiev,²⁶ C. Aidala,³⁴ N.N. Ajitanand,⁵⁴ Y. Akiba,^{48,49} R. Akimoto,¹⁰ H. Al-Ta'ani,⁴³ J. Alexander,⁵⁴ A. Angerami,¹² K. Aoki,⁴⁸ N. Apadula,⁵⁵ Y. Aramaki,^{10,48} H. Asano,^{31,48} E.C. Aschenauer,⁶ E.T. Atomssa,⁵⁵ T.C. Awes,⁴⁵ B. Azmoun,⁶ V. Babintsev,²² M. Bai,⁵ B. Bannier,⁵⁵ K.N. Barish,⁷ B. Bassalleck,⁴² S. Bathe,^{4,49} V. Baublis,⁴⁷ S. Baumgart,⁴⁸ A. Bazilevsky,⁶ R. Belmont,⁵⁹ A. Berdnikov,⁵¹ Y. Berdnikov,⁵¹ X. Bing,⁴⁴ D.S. Blau,³⁰ K. Boyle,⁴⁹ M.L. Brooks,³⁴ H. Buesching,⁶ V. Bumazhnov,²² S. Butsyk,⁴² S. Campbell,⁵⁵ P. Castera,⁵⁵ C.-H. Chen,⁵⁵ C.Y. Chi,¹² M. Chiu,⁶ I.J. Choi,²³ J.B. Choi,⁹ S. Choi,⁵³ R.K. Choudhury,³ P. Christiansen,³⁶ T. Chujo,⁵⁸ O. Chvala,⁷ V. Cianciolo,⁴⁵ Z. Citron,⁵⁵ B.A. Cole,¹² M. Connors,⁵⁵ M. Csanád,¹⁶ T. Csörgő,⁶¹ S. Dairaku,^{31,48} A. Datta,³⁸ M.S. Daugherty,¹ G. David,⁶ A. Denisov,²² A. Deshpande,^{49,55} E.J. Desmond,⁶ K.V. Dharmawardane,⁴³ O. Dietzsch,⁵² L. Ding,²⁵ A. Dion,²⁵ M. Donadelli,⁵² O. Drapier,³² A. Drees,⁵⁵ K.A. Drees,⁵ J.M. Durham,⁵⁵ A. Durum,²² L. D'Orazio,³⁷ S. Edwards,⁵ Y.V. Efremenko,⁴⁵ T. Engelmores,¹² A. Enokizono,⁴⁵ S. Esumi,⁵⁸ K.O. Eyster,⁷ B. Fadem,³⁹ D.E. Fields,⁴² M. Finger,⁸ M. Finger, Jr.,⁸ F. Fleuret,³² S.L. Fokin,³⁰ J.E. Frantz,⁴⁴ A. Franz,⁶ A.D. Frawley,¹⁸ Y. Fukao,⁴⁸ T. Fusayasu,⁴¹ K. Gainey,¹ C. Gal,⁵⁵ A. Garishvili,⁵⁶ I. Garishvili,³³ A. Glenn,³³ X. Gong,⁵⁴ M. Gonin,³² Y. Goto,^{48,49} R. Granier de Cassagnac,³² N. Grau,¹² S.V. Greene,⁵⁹ M. Grosse Perdekamp,²³ T. Gunji,¹⁰ L. Guo,³⁴ H.-Å. Gustafsson,^{36,*} T. Hachiya,⁴⁸ J.S. Haggerty,⁶ K.I. Hahn,¹⁷ H. Hamagaki,¹⁰ J. Hanks,¹² K. Hashimoto,^{48,50} E. Haslum,³⁶ R. Hayano,¹⁰ X. He,¹⁹ T.K. Hemmick,⁵⁵ T. Hester,⁷ J.C. Hill,²⁵ R.S. Hollis,⁷ K. Homma,²¹ B. Hong,²⁹ T. Horaguchi,⁵⁸ Y. Hori,¹⁰ S. Huang,⁵⁹ T. Ichihara,^{48,49} H. Iinuma,²⁸ Y. Ikeda,^{48,58} J. Imrek,¹⁵ M. Inaba,⁵⁸ A. Iordanova,⁷ D. Isenhower,¹ M. Issah,⁵⁹ A. Isupov,²⁶ D. Ivanischev,⁴⁷ B.V. Jacak,^{55,†} M. Javani,¹⁹ J. Jia,^{6,54} X. Jiang,³⁴ B.M. Johnson,⁶ K.S. Joo,⁴⁰ D. Jouan,⁴⁶ J. Kamin,⁵⁵ S. Kaneti,⁵⁵ B.H. Kang,²⁰ J.H. Kang,⁶² J.S. Kang,²⁰ J. Kapustinsky,³⁴ K. Karatsu,^{31,48} M. Kasai,^{48,50} D. Kawall,^{38,49} A.V. Kazantsev,³⁰ T. Kempel,²⁵ A. Khanzadeev,⁴⁷ K.M. Kijima,²¹ B.I. Kim,²⁹ C. Kim,²⁹ D.J. Kim,²⁷ E.J. Kim,⁹ H.J. Kim,⁶² K.-B. Kim,⁶³ Y.-J. Kim,²³ Y.K. Kim,²⁰ E. Kinney,¹¹ Á. Kiss,¹⁶ E. Kistenev,⁶ J. Klatsky,¹⁸ D. Kleinjan,⁷ P. Kline,⁵⁵ Y. Komatsu,¹⁰ B. Komkov,⁴⁷ J. Koster,²³ D. Kotchetkov,⁴⁴ D. Kotov,⁵¹ A. Král,¹³ F. Krizek,²⁷ G.J. Kunde,³⁴ K. Kurita,^{48,50} M. Kurosawa,⁴⁸ Y. Kwon,⁶² G.S. Kyle,⁴³ R. Lacey,⁵⁴ Y.S. Lai,¹² J.G. Lajoie,²⁵ A. Lebedev,²⁵ B. Lee,²⁰ D.M. Lee,³⁴ J. Lee,¹⁷ K.B. Lee,²⁹ K.S. Lee,²⁹ S.H. Lee,⁵⁵ S.R. Lee,⁹ M.J. Leitch,³⁴ M.A.L. Leite,⁵² M. Leitgab,²³ B. Lewis,⁵⁵ S.H. Lim,⁶² L.A. Linden Levy,¹¹ A. Litvinenko,²⁶ M.X. Liu,³⁴ B. Love,⁵⁹ C.F. Maguire,⁵⁹ Y.I. Makdisi,⁵ M. Makek,⁶⁰ A. Malakhov,²⁶ A. Manion,⁵⁵ V.I. Manko,³⁰ E. Mannel,¹² S. Masumoto,¹⁰ M. McCumber,¹¹ P.L. McGaughey,³⁴ D. McGlinchey,¹⁸ C. McKinney,²³ M. Mendoza,⁷ B. Meredith,²³ Y. Miake,⁵⁸ T. Mibe,²⁸ A.C. Mignerey,³⁷ A. Milov,⁶⁰ D.K. Mishra,³ J.T. Mitchell,⁶ Y. Miyachi,^{48,57} S. Miyasaka,^{48,57} A.K. Mohanty,³ H.J. Moon,⁴⁰ D.P. Morrison,⁶ S. Motschwiller,³⁹ T.V. Moukhanova,³⁰ T. Murakami,^{31,48} J. Murata,^{48,50} T. Nagae,³¹ S. Nagamiya,²⁸ J.L. Nagle,¹¹ M.I. Nagy,⁶¹ I. Nakagawa,^{48,49} Y. Nakamiya,²¹ K.R. Nakamura,^{31,48} T. Nakamura,⁴⁸ K. Nakano,^{48,57} C. Nattrass,⁵⁶ A. Nederlof,³⁹ M. Nishihashi,^{21,48} R. Nouicer,^{6,49} N. Novitzky,²⁷ A.S. Nyanin,³⁰ E. O'Brien,⁶ C.A. Ogilvie,²⁵ K. Okada,⁴⁹ A. Oskarsson,³⁶ M. Ouchida,^{21,48} K. Ozawa,¹⁰ R. Pak,⁶ V. Papavassiliou,⁴³ B.H. Park,²⁰ I.H. Park,¹⁷ S.K. Park,²⁹ S.F. Pate,⁴³ L. Patel,¹⁹ H. Pei,²⁵ J.-C. Peng,²³ H. Pereira,¹⁴ V. Peresedov,²⁶ D.Yu. Peressounko,³⁰ R. Petti,⁵⁵ C. Pinkenburg,⁶ R.P. Pisani,⁶ M. Proissl,⁵⁵ M.L. Purschke,⁶ H. Qu,¹ J. Rak,²⁷ I. Ravinovich,⁶⁰ K.F. Read,^{45,56} R. Reynolds,⁵⁴ V. Riabov,⁴⁷ Y. Riabov,⁴⁷ E. Richardson,³⁷ D. Roach,⁵⁹ G. Roche,³⁵ S.D. Rolnick,⁷ M. Rosati,²⁵ P. Rukoyatkin,²⁶ B. Sahlmueller,⁵⁵ N. Saito,²⁸ T. Sakaguchi,⁶ V. Samsonov,⁴⁷ M. Sano,⁵⁸ M. Sarsour,¹⁹ S. Sawada,²⁸ K. Sedgwick,⁷ R. Seidl,^{48,49} A. Sen,¹⁹ R. Seto,⁷ D. Sharma,⁶⁰ I. Shein,²² T.-A. Shibata,^{48,57} K. Shigaki,²¹ M. Shimomura,⁵⁸ K. Shoji,^{31,48} P. Shukla,³ A. Sickles,⁶ C.L. Silva,²⁵ D. Silvermyr,⁴⁵ K.S. Sim,²⁹ B.K. Singh,² C.P. Singh,² V. Singh,² M. Slunečka,⁸ R.A. Soltz,³³ W.E. Sondheim,³⁴ S.P. Sorensen,⁵⁶ M. Soumya,⁵⁴ I.V. Sourikova,⁶ P.W. Stankus,⁴⁵ E. Stenlund,³⁶ M. Stepanov,³⁸ A. Ster,⁶¹ S.P. Stoll,⁶ T. Sugitate,²¹ A. Sukhanov,⁶ J. Sun,⁵⁵ J. Sziklai,⁶¹ E.M. Takagui,⁵² A. Takahara,¹⁰ A. Taketani,^{48,49} Y. Tanaka,⁴¹ S. Taneja,⁵⁵ K. Tanida,^{49,53} M.J. Tannenbaum,⁶ S. Tarafdar,² A. Taranenko,⁵⁴ E. Tennant,⁴³ H. Themann,⁵⁵ T. Todoroki,^{48,58} L. Tomášek,²⁴ M. Tomášek,^{13,24} H. Torii,²¹ R.S. Towell,¹ I. Tserruya,⁶⁰ Y. Tsuchimoto,¹⁰ T. Tsuji,¹⁰ C. Vale,⁶ H.W. van Hecke,³⁴ M. Vargyas,¹⁶ E. Vazquez-Zambrano,¹² A. Veicht,¹² J. Velkovska,⁵⁹ R. Vértesi,⁶¹ M. Virius,¹³ A. Vossen,²³ V. Vrba,^{13,24} E. Vznuzdaev,⁴⁷ X.R. Wang,⁴³ D. Watanabe,²¹ K. Watanabe,⁵⁸ Y. Watanabe,^{48,49} Y.S. Watanabe,¹⁰ F. Wei,²⁵ R. Wei,⁵⁴ S.N. White,⁶ D. Winter,¹² S. Wolin,²³ C.L. Woody,⁶ M. Wysocki,¹¹ Y.L. Yamaguchi,¹⁰ R. Yang,²³ A. Yanovich,²² J. Ying,¹⁹ S. Yokkaichi,^{48,49} Z. You,³⁴ I. Younus,⁴² I.E. Yushmanov,³⁰ W.A. Zajc,¹² A. Zelenski,⁵ and L. Zolin²⁶

(PHENIX Collaboration)

- ¹Abilene Christian University, Abilene, Texas 79699, USA
²Department of Physics, Banaras Hindu University, Varanasi 221005, India
³Bhabha Atomic Research Centre, Bombay 400 085, India
⁴Baruch College, City University of New York, New York, New York, 10010 USA
⁵Collider-Accelerator Department, Brookhaven National Laboratory, Upton, New York 11973-5000, USA
⁶Physics Department, Brookhaven National Laboratory, Upton, New York 11973-5000, USA
⁷University of California - Riverside, Riverside, California 92521, USA
⁸Charles University, Ovocný trh 5, Praha 1, 116 36, Prague, Czech Republic
⁹Chonbuk National University, Jeonju, 561-756, Korea
¹⁰Center for Nuclear Study, Graduate School of Science, University of Tokyo, 7-3-1 Hongo, Bunkyo, Tokyo 113-0033, Japan
¹¹University of Colorado, Boulder, Colorado 80309, USA
¹²Columbia University, New York, New York 10027 and Nevis Laboratories, Irvington, New York 10533, USA
¹³Czech Technical University, Zikova 4, 166 36 Prague 6, Czech Republic
¹⁴Dapnia, CEA Saclay, F-91191, Gif-sur-Yvette, France
¹⁵Debrecen University, H-4010 Debrecen, Egyetem tér 1, Hungary
¹⁶ELTE, Eötvös Loránd University, H - 1117 Budapest, Pázmány P. s. 1/A, Hungary
¹⁷Ewha Womans University, Seoul 120-750, Korea
¹⁸Florida State University, Tallahassee, Florida 32306, USA
¹⁹Georgia State University, Atlanta, Georgia 30303, USA
²⁰Hanyang University, Seoul 133-792, Korea
²¹Hiroshima University, Kagamiyama, Higashi-Hiroshima 739-8526, Japan
²²IHEP Protvino, State Research Center of Russian Federation, Institute for High Energy Physics, Protvino, 142281, Russia
²³University of Illinois at Urbana-Champaign, Urbana, Illinois 61801, USA
²⁴Institute of Physics, Academy of Sciences of the Czech Republic, Na Slovance 2, 182 21 Prague 8, Czech Republic
²⁵Iowa State University, Ames, Iowa 50011, USA
²⁶Joint Institute for Nuclear Research, 141980 Dubna, Moscow Region, Russia
²⁷Helsinki Institute of Physics and University of Jyväskylä, P.O.Box 35, FI-40014 Jyväskylä, Finland
²⁸KEK, High Energy Accelerator Research Organization, Tsukuba, Ibaraki 305-0801, Japan
²⁹Korea University, Seoul, 136-701, Korea
³⁰Russian Research Center "Kurchatov Institute", Moscow, 123098 Russia
³¹Kyoto University, Kyoto 606-8502, Japan
³²Laboratoire Leprince-Ringuet, Ecole Polytechnique, CNRS-IN2P3, Route de Saclay, F-91128, Palaiseau, France
³³Lawrence Livermore National Laboratory, Livermore, California 94550, USA
³⁴Los Alamos National Laboratory, Los Alamos, New Mexico 87545, USA
³⁵LPC, Université Blaise Pascal, CNRS-IN2P3, Clermont-Fd, 63177 Aubiere Cedex, France
³⁶Department of Physics, Lund University, Box 118, SE-221 00 Lund, Sweden
³⁷University of Maryland, College Park, Maryland 20742, USA
³⁸Department of Physics, University of Massachusetts, Amherst, Massachusetts 01003-9337, USA
³⁹Muhlenberg College, Allentown, Pennsylvania 18104-5586, USA
⁴⁰Myongji University, Yongin, Kyonggido 449-728, Korea
⁴¹Nagasaki Institute of Applied Science, Nagasaki-shi, Nagasaki 851-0193, Japan
⁴²University of New Mexico, Albuquerque, New Mexico 87131, USA
⁴³New Mexico State University, Las Cruces, New Mexico 88003, USA
⁴⁴Department of Physics and Astronomy, Ohio University, Athens, Ohio 45701, USA
⁴⁵Oak Ridge National Laboratory, Oak Ridge, Tennessee 37831, USA
⁴⁶IPN-Orsay, Université Paris Sud, CNRS-IN2P3, BP1, F-91406, Orsay, France
⁴⁷PNPI, Petersburg Nuclear Physics Institute, Gatchina, Leningrad region, 188300, Russia
⁴⁸RIKEN Nishina Center for Accelerator-Based Science, Wako, Saitama 351-0198, Japan
⁴⁹RIKEN BNL Research Center, Brookhaven National Laboratory, Upton, New York 11973-5000, USA
⁵⁰Physics Department, Rikkyo University, 3-34-1 Nishi-Ikebukuro, Toshima, Tokyo 171-8501, Japan
⁵¹Saint Petersburg State Polytechnic University, St. Petersburg, 195251 Russia
⁵²Universidade de São Paulo, Instituto de Física, Caixa Postal 66318, São Paulo CEP05315-970, Brazil
⁵³Department of Physics and Astronomy, Seoul National University, Seoul, Korea
⁵⁴Chemistry Department, Stony Brook University, SUNY, Stony Brook, New York 11794-3400, USA
⁵⁵Department of Physics and Astronomy, Stony Brook University, SUNY, Stony Brook, New York 11794-3400, USA
⁵⁶University of Tennessee, Knoxville, Tennessee 37996, USA
⁵⁷Department of Physics, Tokyo Institute of Technology, Oh-okayama, Meguro, Tokyo 152-8551, Japan
⁵⁸Institute of Physics, University of Tsukuba, Tsukuba, Ibaraki 305, Japan
⁵⁹Vanderbilt University, Nashville, Tennessee 37235, USA
⁶⁰Weizmann Institute, Rehovot 76100, Israel
⁶¹Institute for Particle and Nuclear Physics, Wigner Research Centre for Physics, Hungarian Academy of Sciences (Wigner RCP, RMKI) H-1525 Budapest 114, POBox 49, Budapest, Hungary

⁶²Yonsei University, IPAP, Seoul 120-749, Korea
⁶³Chonbuk

(Dated: February 4, 2021)

Neutral-pion, π^0 , spectra were measured at midrapidity ($|y| < 0.35$) in Au+Au collisions at $\sqrt{s_{NN}} = 39$ and 62.4 GeV and compared to earlier measurements at 200 GeV in the $1 < p_T < 10$ GeV/ c transverse-momentum (p_T) range. The high- p_T tail is well described by a power law in all cases and the powers decrease significantly with decreasing center-of-mass energy. The change of powers is very similar to that observed in the corresponding $p+p$ -collision spectra. The nuclear-modification factors (R_{AA}) show significant suppression and a distinct energy dependence at moderate p_T in central collisions. At high p_T , R_{AA} is similar for 62.4 and 200 GeV at all centralities. Perturbative-quantum-chromodynamics calculations that describe R_{AA} well at 200 GeV, fail to describe the 39 GeV data, raising the possibility that the relative importance of initial-state effects and soft processes increases at lower energies. A conclusion that the region where hard processes are dominant is reached only at higher p_T , is also supported by the x_T dependence of the x_T -scaling power-law exponent.

PACS numbers: 25.75.Dw

Large transverse-momentum (p_T) particles produced in high-energy nucleus-nucleus (AB) collisions play a crucial role in studying the properties of the medium created in relativistic heavy-ion collisions. Most hadrons at sufficiently high p_T are fragmentation products of hard-scattered partons and their production rate in vacuum, as measured in $p+p$ collisions, is well described by perturbative quantum chromodynamics (pQCD) [1]. In the absence of any nuclear effects the production rate in relativistic heavy-ion collisions in the pQCD regime, i.e. at sufficiently high p_T , would scale with the increased probability that a hard scattering occurs, due to the large number of nucleons. This probability is characterized by the nuclear thickness function T_{AB} [2]. However, such scaling has been violated to various degrees depending both on collision energy, $\sqrt{s_{NN}}$, and hadron p_T . At lower collision energies, the hadron yield is enhanced above the expected scaling. This was first observed in $p+A$ and this enhancement is generally attributed to multiple soft scattering (“Cronin effect” [3]), and is presumed to occur in ion-ion collisions as well. Initial parton distribution functions in nuclei (nPDF) are different from those in protons [4].

Finally, if a dense, colored medium is formed in the AB collision, the hard-scattered parton may traverse some of it, losing energy in the process. Therefore, the observed yield at a given (high) p_T will be lower than that expected from T_{AB} scaling, exhibiting “suppression” or “jet quenching,” described in terms of the nuclear-modification factor, R_{AA} (see Eq. (1)). Alternatively, other studies divide the yields for heavy-ion collisions at one energy with those for the same colliding species at a lower energy Au+Au, rather than scaled $p+p$ reference data, to study energy and centrality scaling [5].

One of the first discoveries at the Relativistic Heavy-Ion Collider (RHIC) was a very large hadron suppression at high p_T (above ≈ 3 GeV/ c) in $\sqrt{s_{NN}} = 130$ and 200 GeV Au+Au collisions [6–9]. This suppression was attributed to the dominance of parton energy loss in the medium, i.e. to final state effects. To test this hypothesis, the same

measurements were performed in $d+Au$ collisions [10], where the formation of the hot, dense partonic medium is not expected, and initial-state effects (if any) prevail. No suppression in $d+Au$ data was observed leaving little (if any) room for the initial-state effects as the origin of the large jet quenching observed in Au + Au. Studies with the lighter Cu+Cu system at three energies ($\sqrt{s_{NN}} = 22.4, 62.4$ and 200 GeV [11]) have revealed that at $\sqrt{s_{NN}} = 22.4$ GeV mechanisms that enhance R_{AA} (> 1) dominate at all centralities. Note, however, that this data set had very limited p_T range ($p_T < 4$ GeV/ c). At 62.4 GeV, jet quenching overwhelms any enhancement and leads to a suppression ($R_{AA} < 1$) in more central collisions.

The low-energy scan at RHIC provides an opportunity to study the transition from enhancement ($R_{AA} > 1$) to suppression ($R_{AA} < 1$) and the evolution of R_{AA} with collision energy, centrality and p_T . The results put constraints on energy-loss models (see [12] and references therein).

Here, we present new measurements by the PHENIX experiment at RHIC of π^0 invariant yields and R_{AA} in Au + Au collisions at $\sqrt{s_{NN}} = 39$ and 62.4 GeV. The data were taken during the 2010 run and the p_T limits (statistics) were 8 GeV/ c and 10 GeV/ c , respectively. Reference $p+p$ -collision data for $\sqrt{s_{NN}} = 62.4$ GeV were taken in the same experiment in the 2006 run [1], while for $\sqrt{s_{NN}} = 39$ GeV, data measured in the FERMILAB experiment E706 were used [13].

Neutral pions were measured on a statistical basis via their $\pi^0 \rightarrow \gamma\gamma$ decay branch with the electromagnetic calorimeter (EMCal) [14]. The EMCal comprises two calorimeter types: 6 sectors of lead scintillator sampling calorimeter (PbSc) and 2 sectors of lead glass Čerenkov calorimeter (PbGl). Each sector is located ≈ 5 m from the beamline and subtends $|\eta| < 0.35$ in pseudorapidity and $\Delta\phi = 22.5^\circ$ in azimuth. This Letter presents results obtained with the PbSc sectors only. The segmentation of the PbSc ($\Delta\eta \times \Delta\phi = 0.01 \times 0.01$) ensures that the two photons from the $\pi^0 \rightarrow \gamma\gamma$ decays are very well resolved

up to $p_T < 12 \text{ GeV}/c$, i.e. across the entire p_T range of this measurement.

The results are based on data sets of $3.5 \cdot 10^8$ and $7.0 \cdot 10^8$ minimum bias Au + Au events at 39 and 62.4 GeV, respectively. The minimum bias (MB) trigger for both $\sqrt{s_{NN}} = 39$ and 62.4 GeV was provided by the Beam-Beam-Counters (BBC) [15], located close to the beam axis in both directions and covering $3.0 \leq |\eta| \leq 3.9$. In order to reduce background at least two hits were required in both BBC's. This condition selects $\sim 86\%$ of the total inelastic cross section. The centrality selection in Au + Au collisions at both energies was based on the charged signal sum of the BBC's, which is proportional to the charged particle multiplicity. For each centrality the average number of binary collisions ($\langle N_{\text{coll}} \rangle$) and the number of participants ($\langle N_{\text{part}} \rangle$) were calculated using a Glauber model [2] based Monte Carlo code.

TABLE I: Sources of systematic uncertainties and their relative effect (in %) on the invariant yields

p_T energy	2 GeV/c		5 GeV/c		Type
	39 GeV	(62.4 GeV)	39 GeV	(62.4 GeV)	
Yield extraction	3%	(3%)	3%	(3%)	A
PID efficiency	4.5%	(4.5%)	4.5%	(4.5%)	B
Energy scale	10.5%	(8.0%)	14.5%	(10.0%)	B
Acceptance	2%	(2%)	2%	(2%)	B
Conversion	4%	(4%)	4%	(4%)	B
Off vertex	1.5%	(1.5%)	1.5%	(1.5%)	C
Total for π^0 yields	12.7%	(10.7%)	16.2%	(12.3%)	

The PHENIX analysis of neutral pions is described in detail elsewhere [9]. Table I lists the sources of systematic uncertainties on the extracted- π^0 invariant yields in this analysis. They can be divided into three different categories: (1) Type-A, p_T -uncorrelated; (2) Type-B, p_T -correlated, where the correlation may be an arbitrary smooth function; (3) Type-C, p_T -correlated, where all points move by the same fraction up or down. The main sources of systematic uncertainties in the π^0 measurement are the energy scale, yield extraction and particle-identification (PID) efficiency correction.

Figure 1 shows the invariant yields of the π^0 s for all centralities and also in minimum bias collisions. From fitting the $\sqrt{s_{NN}} = 39$ and 62.4 GeV minimum bias spectra with a power law function ($\propto p_T^n$) for $p_T > 4 \text{ GeV}/c$, we obtained powers $n_{39} = -13.04 \pm 0.08$ and $n_{62.4} = -10.60 \pm 0.03$, respectively, significantly steeper than at $\sqrt{s_{NN}} = 200 \text{ GeV}$, where $n_{200} = -8.06 \pm 0.01$ for MB collisions [9]. The slopes of the corresponding $p+p$ collision spectra are somewhat different, but comparable, $n_{39}^{pp} = -13.59 \pm 0.21$, $n_{62.4}^{pp} = -9.82 \pm 0.18$ and $n_{200}^{pp} = -8.22 \pm 0.09$, respectively.

Nuclear effects on the π^0 production are quantified us-

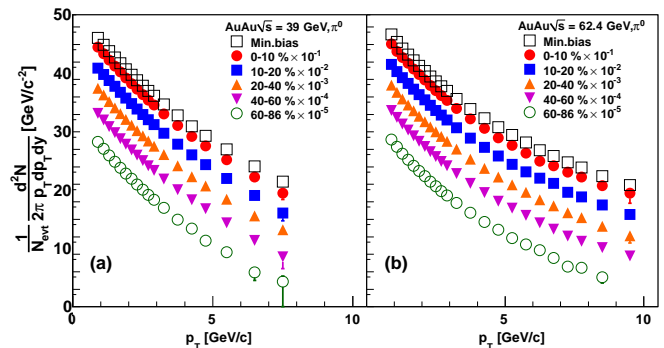


FIG. 1: (Color online) Invariant yields of π^0 in Au + Au at $\sqrt{s_{NN}} = 39 \text{ GeV}$ (a) and 62.4 GeV (b) in all centralities and minimum bias. Only statistical uncertainties are shown.

ing the nuclear modification factor

$$R_{AA}(p_T) = \frac{(1/N_{AA}^{\text{evt}})d^2N_{AA}^{\pi^0}/dp_T dy}{\langle T_{AB} \rangle \times d^2\sigma_{pp}^{\pi^0}/dp_T dy}, \quad (1)$$

where $\sigma_{pp}^{\pi^0}$ is the production cross section of π^0 in $p+p$ collisions, and $\langle T_{AB} \rangle = \langle N_{\text{coll}} \rangle / \sigma_{pp}^{\text{inel}}$ is the nuclear thickness function averaged over the range of impact parameters contributing to the given centrality class according to the Glauber model. Thus R_{AA} compares the yield observed in $A + A$ collisions to the yield expected from the superposition of N_{coll} independent $p+p$ interactions. In the absence of nuclear effects, R_{AA} should be equal to unity. However, $R_{AA} \approx 1$ does not necessarily imply the absence of suppression, it may also indicate a balance between enhancing and depleting mechanisms.

In order to calculate R_{AA} , a reference p_T distribution in $p+p$ collisions is needed. Preferably this is measured with the same detector, in which case many systematic uncertainties cancel in the ratio. The PHENIX experiment has measured the π^0 cross section in $p+p$ collisions at $\sqrt{s_{NN}} = 62.4 \text{ GeV}$ [1] but only up to $p_T = 7 \text{ GeV}/c$ while the current Au+Au measurement reaches up to $10 \text{ GeV}/c$. Hence the $p+p$ data were fitted with a power law function between $4.5 < p_T < 7 \text{ GeV}/c$ and then extrapolated. The systematic uncertainty resulting from this extrapolation reaches 20% at $10 \text{ GeV}/c$, estimated from a series of fits, where each time one or more randomly selected points are omitted and the remaining points are re-fitted.

So far PHENIX has not measured the $p+p$ spectrum of π^0 at $\sqrt{s_{NN}} = 39 \text{ GeV}$. Therefore, data from the Fermilab experiment E706 [13] were used. However, the E706 acceptance ($-1. < |\eta| < 0.5$) is different from that of PHENIX ($|\eta| < 0.35$), and since $dN/d\eta$ is not flat, a p_T -dependent correction was applied to the E706 data. This correction factor was determined from a PYTHIA simulation by means of the ratio of yields (normalized per unit rapidity) when calculated from the observed yield in the

PHENIX and E706 acceptance windows. The systematic uncertainty of the correction is 1–2% at 3 GeV/ c but reaches 20% at 8 GeV/ c .

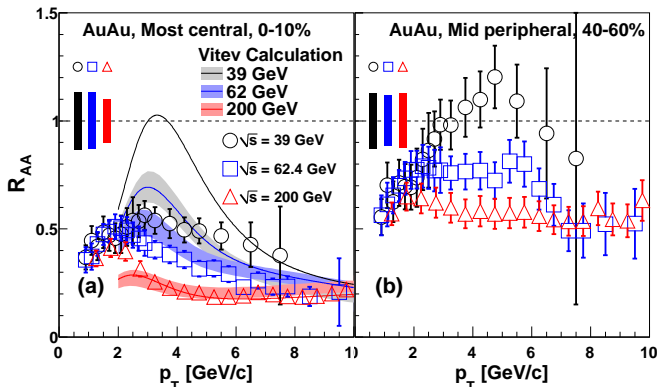


FIG. 2: (Color online) Nuclear modification factor (R_{AA}) of π^0 in Au + Au collisions in most central 0–10% (a) and mid-peripheral 40–60% (b). Error bars are the quadratic sum of statistical and p_T -correlated systematic uncertainties (including systematic uncertainties from the $p+p$ -collision reference). Boxes around 1 are the quadratic sum of the C-type uncertainties combined with the N_{coll} uncertainties. These are fully correlated between different energies. Also shown for central collisions are pQCD calculations [16] with regular Cronin-effect (solid lines) and with the Cronin-effect reduced by a factor of two for all three energies (bands).

Figure 2 shows the nuclear modification factor of π^0 s measured in Au + Au collisions at $\sqrt{s_{NN}} = 39, 62.4$ and 200 GeV (data from [9]) as a function of p_T for most central collisions (a) and 40–60% centrality (b). In the most central collisions (0–10%) there is a significant suppression for all three energies, while in mid-peripheral collisions (40–60%) at $\sqrt{s_{NN}} = 39$ GeV, R_{AA} is consistent with unity above $p_T > 3$ GeV/ c .

For 0–10% pQCD calculations [16, 17] are also shown. The solid curves are calculated with the same parametrization that was successful for 200 GeV Au + Au data (and also 200 GeV Cu + Cu [11]). Neither the 62.4, nor the 39 GeV data are consistent with the predictions. The only qualitative agreement is that the turnover point of the R_{AA} curves moves to higher p_T with lower collision energy as observed in the data. The bands are calculated within the same framework but with the Cronin-effect reduced and the energy loss varied by $\pm 10\%$. The 200 GeV data are still well described, the 62.4 GeV data are consistent within uncertainties, but the 39 GeV R_{AA} , particularly the shape, is inconsistent with the corresponding band.

Coupled with the observations that the slopes at high p_T become much steeper, but the bulk properties (like elliptic flow, energy density, apparent temperature) change only slowly in the collision energy range in question, it is quite conceivable that hard scattering as a source of par-

ticles at a given p_T becomes completely dominant only at higher transverse momentum, i.e. jet quenching will be “masked” up to higher p_T . Note that while the shapes at lower p_T are different, at $p_T \gtrsim 7$ GeV/ c R_{AA} is essentially the same for the 62.4 and 200 GeV data, irrespective of centrality (see also Fig. 3). While in the 39 GeV data R_{AA} also shows a decreasing trend at higher p_T , unfortunately the p_T reach of the current data sample precludes any conclusion as to what would happen to their R_{AA} at even higher p_T .

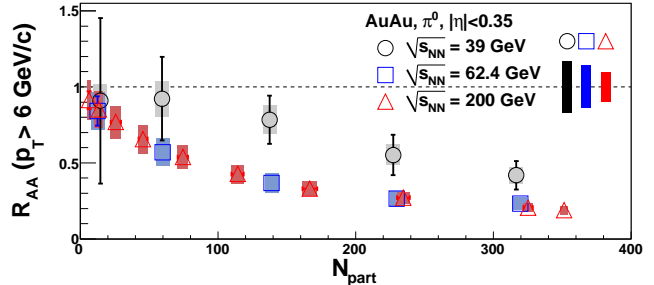


FIG. 3: (Color online) Nuclear modification factor averaged for $p_T > 6$ GeV/ c . Uncertainties are shown as error bars (statistical), boxes (sum of p_T -uncorrelated and N_{coll}), boxes around one (Type B and C and uncertainties from the $p+p$ -collision reference).

Figure 3 shows p_T -averaged R_{AA} as a function of the number of participants. The averaging was done above $p_T > 6$ GeV/ c . Our first observation is that R_{AA} decreases with increasing centrality even for the lowest-energy system. Similarly, as already discussed in the context of Fig. 2, at high enough p_T the suppression is the same at 62.4 and 200 GeV, at all centralities. This is remarkable because the power n of the fit to the spectra changes approximately by two units from 200 to 62.4 GeV, so the average momentum loss of the partons also has to be different in order to compensate the effect of the changing slope. The average momentum loss is usually defined by the fractional momentum shift $\delta p_T/p_T$ between the corresponding Au + Au and T_{AA} -scaled $p+p$ spectra as follows. Since the power law tails of the $p+p$ and Au + Au spectra are similar, they can be fitted simultaneously with the same function and same power n

$$f(p_T) = \frac{A}{(p_T(1 + \delta p_T/p_T))^n} \quad (2)$$

with δp_T being the horizontal shift between the scaled $p+p$ and the Au + Au spectra. In panel (a) of Fig. 4, the observed fractional momentum shifts are shown for central collisions, as a function of the Au + Au p_T .

Inclusive single-particle spectra at sufficiently high p_T and collision energy were predicted to exhibit scaling with the variable $x_T = 2p_T/\sqrt{s}$ such that the produc-

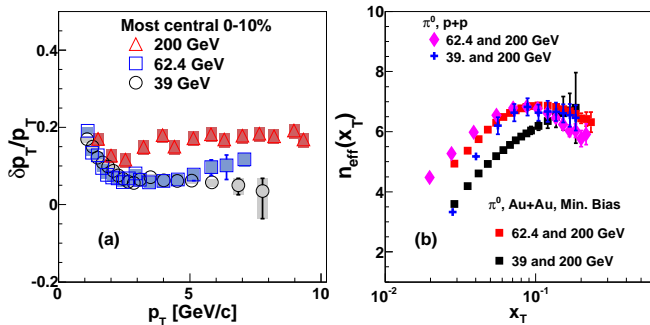


FIG. 4: (Color online) (a) Fractional momentum shift $\delta p_T/p_T$ between Au + Au and T_{AA} -scaled $p+p$ data as a function of the Au + Au p_T . (b) Power n_{eff} of x_T -scaling for $p+p$ and Au + Au (minimum bias) at various collision energies.

tion cross section can be written in a form [18, 19]

$$E \frac{d^3\sigma}{dp^3} = \frac{1}{\sqrt{s}^{n(x_T, \sqrt{s})}} G(x_T) \quad (3)$$

where $G(x_T)$ is a universal function and $n(x_T, \sqrt{s})$ characterizes the specific process [19]. The scaling power $n_{\text{eff}}(x_T)$ between any pair of $\sqrt{s_{NN}}$ energies is then calculated as

$$n_{\text{eff}}(x_T) = \frac{\log(\text{Yield}(x_T, \sqrt{s_1})/\text{Yield}(x_T, \sqrt{s_2}))}{\log(\sqrt{s_2}/\sqrt{s_1})} \quad (4)$$

In panel (b) of Fig. 4, $n_{\text{eff}}(x_T)$ is shown when comparing invariant- π^0 yields in $p+p$ and Au + Au collisions at different energies. Both the shape and the magnitude of $n_{\text{eff}}(x_T)$ is similar for the 62.4/200 GeV $p+p$ and Au + Au as well as for the 39/200 GeV $p+p$ data. The rise of $n_{\text{eff}}(x_T)$ at lower x_T can be attributed to the dominance of soft processes [20], while at higher x_T they deviate strongly from leading-twist scaling predictions [19, 21]. However, the shape of $n_{\text{eff}}(x_T)$ in the 39 and 200 GeV Au + Au comparison is very different from all others. It may not even reach its maximum in the measured x_T range, and its constant rise is similar to the rise observed in the low- x_T (soft) region of the other data shown. One possible explanation could be that while present, hard scattering is still not the overwhelming source of high- p_T π^0 s in the currently available p_T range in 39 GeV Au + Au collisions.

In summary, the π^0 p_T spectra were measured in Au + Au collisions at two different energies, $\sqrt{s_{NN}} = 39$ and 62.4 GeV, and compared to the earlier result for $\sqrt{s_{NN}} = 200$ GeV. In all cases the high p_T part of the invariant yields can be well described with a single power law function. The powers decrease considerably at lower $\sqrt{s_{NN}}$, and since the soft processes change only slowly with collision energy, jet quenching might be “masked” up to higher transverse momenta. The high- p_T π^0 yields in Au + Au at 62.4 GeV are suppressed,

and above $p_T > 6$ GeV/ c the data points are comparable with the 200 GeV results at all centralities. The π^0 yields in Au + Au at 39 GeV are suppressed in the most central collisions, but no suppression is apparent in more peripheral collisions. At lower energies, a decreasing momentum shift compensates for the steeper slopes at high p_T , making the R_{AA} ’s comparable, in fact, identical in the case of 62.4 and 200 GeV. When related to 200 GeV, $n_{\text{eff}}(x_T)$ is similar for 62.4 and 39 GeV $p+p$ and 62.4 GeV Au + Au, but very different for the 39 GeV Au + Au data. The new data provided in a wide energy range of Au + Au collisions will help to constrain energy-loss models.

We thank the staff of the Collider-Accelerator and Physics Departments at Brookhaven National Laboratory and the staff of the other PHENIX participating institutions for their vital contributions. We acknowledge support from the Office of Nuclear Physics in the Office of Science of the Department of Energy, the National Science Foundation, Abilene Christian University Research Council, Research Foundation of SUNY, and Dean of the College of Arts and Sciences, Vanderbilt University (U.S.A), Ministry of Education, Culture, Sports, Science, and Technology and the Japan Society for the Promotion of Science (Japan), Conselho Nacional de Desenvolvimento Científico e Tecnológico and Fundação de Amparo à Pesquisa do Estado de São Paulo (Brazil), Natural Science Foundation of China (P. R. China), Ministry of Education, Youth and Sports (Czech Republic), Jyväskylä University (Finland), Centre National de la Recherche Scientifique, Commissariat à l’Énergie Atomique, and Institut National de Physique Nucléaire et de Physique des Particules (France), Ministry of Industry, Science and Technologies, Bundesministerium für Bildung und Forschung, Deutscher Akademischer Austausch Dienst, and Alexander von Humboldt Stiftung (Germany), Hungarian National Science Fund, OTKA (Hungary), Department of Atomic Energy and Department of Science and Technology (India), Israel Science Foundation (Israel), National Research Foundation and WCU program of the Ministry Education Science and Technology (Korea), Ministry of Education and Science, Russian Academy of Sciences, Federal Agency of Atomic Energy (Russia), VR and Wallenberg Foundation (Sweden), the U.S. Civilian Research and Development Foundation for the Independent States of the Former Soviet Union, the Hungarian American Enterprise Scholarship Fund, and the US-Israel Binational Science Foundation.

* Deceased

† PHENIX Spokesperson: jacak@skipper.physics.sunysb.edu

- [1] A. Adare et al. (PHENIX Collaboration), Phys. Rev. D **79**, 012003 (2009).
 [2] M. L. Miller, K. Reyers, S. J. Sanders, and P. Steinberg,

- Annu. Rev. Nucl. Part. Sci **57**, 205 (2007).
- [3] J. W. Cronin, H. J. Frisch, and M. J. Shochet, Phys. Rev. D **11**, 3105 (1975).
 - [4] K. Eskola, H. Paukkunen, and C. Salgado, Nucl. Phys. A **855**, 150 (2011), 1011.6534.
 - [5] B. Alver et al. (PHOBOS Collaboration), Phys. Rev. C **80**, 011901 (2009).
 - [6] K. Adcox et al. (PHENIX Collaboration), Phys. Rev. Lett. **88**, 022301 (2002).
 - [7] C. Adler et al. (STAR Collaboration), Phys.Rev.Lett. **89**, 202301 (2002).
 - [8] S. S. Adler et al. (PHENIX Collaboration), Phys. Rev. Lett. **91**, 072301 (2003).
 - [9] A. Adare et al. (PHENIX Collaboration), Phys. Rev. Lett. **101**, 232301 (2008).
 - [10] S. S. Adler et al. (PHENIX Collaboration), Phys. Rev. Lett. **91**, 072303 (2003).
 - [11] A. Adare et al. (PHENIX Collaboration), Phys. Rev. Lett. **101**, 162301 (2008).
 - [12] N. Armesto et al. (2011), 1106.1106.
 - [13] L. Apanasevich et al. (E706 Collaboration), Phys. Rev. D **68**, 052001 (2003).
 - [14] L. Aphecetche et al. (PHENIX Collaboration), Nucl. Instrum. Methods A **499**, 521 (2003).
 - [15] M. Allen et al. (PHENIX Collaboration), Nucl. Instrum. Methods A **499**, 549 (2003).
 - [16] I. Vitev, private communication (2012).
 - [17] R. Sharma, I. Vitev, and B.-W. Zhang, Phys. Rev. C **80**, 054902 (2009).
 - [18] R. Blankenbecler, S. J. Brodsky, and J. F. Gunion, Phys. Lett. B **42**, 461 (1972).
 - [19] S. J. Brodsky, H. J. Pirner, and J. Raufeisenm, Phys. Lett. B **637**, 58 (2006), 0510315.
 - [20] S. M. Berman, J. D. Bjorken, and J. B. Kogut, Phys. Rev. D **4**, 3388 (1971).
 - [21] F. Arleo, S. J. Brodsky, D. S. Hwang, and A. M. Sickles, Phys. Rev. Lett. **105**, 062002 (2010).